Contract No.:

This manuscript has been authored by Savannah River Nuclear Solutions (SRNS), LLC under Contract No. DE-AC09-08SR22470 with the U.S. Department of Energy (DOE) Office of Environmental Management (EM).

The Performance of Underground Radioactive Waste Storage Tanks at the Savannah River Site: A 60-year Historical Perspective

Bruce J. Wiersma, Savannah River National Laboratory

Abstract

The Savannah River Site produced weapons grade materials for nearly 35 years between 1953 and 1988. The legacy of this production is nearly 36 million gallons of radioactive waste. Since the 1950's, the liquid waste has been stored in large, underground carbon steel waste tanks. During the past 20 years the site has begun to process the waste so that it may be stored in vitrified and grout forms, which are more suitable for long term storage. Over the history of the site, some of the tanks have experienced leakage of the waste to the secondary containment. This paper reviews the instances of leakage and corrosion degradation that the tanks and associated equipment have experienced during this time. Furthermore, activities that the site has taken to mitigate the degradation and manage the service life of the tank for its anticipated lifetime are reviewed.

Introduction

The Savannah River Site (SRS) is located in south-central South Carolina, approximately 100 miles from the Atlantic Coast. The major physical feature at SRS is the Savannah River, approximately 20 miles which serves as the southwestern boundary of the site and the South Carolina-Georgia border. SRS encompasses portions of Aiken, Barnwell, and Allendale Counties in South Carolina. SRS occupies an almost circular area of approximately 310 square miles, and contains production, service, and research and development areas (see Figure 1). The developed areas occupy less than 10% of SRS area while the remainder of the site is undeveloped forest or wetlands.

Figure 1. Location of the Savannah River Site

The radioactive wastes are primarily produced from the reprocessing of spent nuclear fuel on site. The waste contains both transuranic waste and fission products in concentrations that require permanent isolation from the environment. The waste originates from two reprocessing facilities on site designated as F-Area and H-Area canyons. Interim storage is of the waste is managed in 45 active, large, shielded underground tanks that are divided between two areas, each associated with one of the canyons. Six of the original 51 waste tanks have been filled with grout and are now closed.

A schematic of the radioactive waste system at SRS is shown in Figure 2. Fresh waste received from the reprocessing canyon is transferred to the waste tanks where it separates into solid (sludge) and liquid (supernate) phases. The supernate is transferred to an evaporator system that reduces the volume of the liquid. As the concentrated supernate cools, salt cake solids crystallize in the bottom of the tanks. Both F- and H-Area tank farms have their own evaporator systems and serve to recover millions of gallons of tank space each year. Without these evaporator systems, SRS would have required 86 additional waste storage tanks to store the waste produced over the site's lifetime.

The site is in the process of closing tanks and has for the past15 years focused on removing the high activity sludge from the tanks. The facility utilizes in-tank processes to prepare the sludge for feed to the Defense Waste Processing Facility (DWPF) by washing the sludge with water to reduce the concentration of soluble sodium salts. The washed sludge is transferred to the DWPF where it is processed by combining with glass frit. The mixture is heated until it melts, and then is poured into stainless steel canisters to cool. The glass-like solid material that forms immobilizes the highly radioactive sludge and seals it off from the environment. The canisters are then stored in a Glass Waste Storage Building (GWSB) until a federal repository is established.

Due to the limited amount of tank space available, some salt waste must be dispositioned to ensure sufficient tank space for continued sludge washing processes. The Actinide Removal Process (ARP) and Modular Caustic Side Solvent Extraction Unit (MCU) work together as an integrated system to remove the radioactive isotopes from salt waste solutions prior to its transfer to the Saltstone Facility.

ARP removes long-lived radioactive contaminants such as plutonium and strontium, by adding mono-sodium titanate (MST) to radioactive salt solutions stored at SRS and then filtering out the MST that has absorbed the radioactive contaminants. The filtering process takes place in the 512-S building. The MST-radionuclide particles are then transferred to DWPF where they are also vitrified. The filtered salt solution is then transferred to the MCU for further processing.

Using a specially engineered solvent, the MCU equipment separates the cesium from the salt solution. The high activity salt solution (i.e., containing cesium) is transferred to the DWPF. The decontaminated salt waste solution is transferred to the Saltstone facility. At the Saltstone facility the salt solution is mixed with cement-like materials to form a grout, which is poured into engineered concrete vaults.

The process of dispositioning the waste began in the mid-1990's. It is anticipated that completion of removal and vitrification of the original 38 million gallons of waste will be completed in the 2030's.

During the history of interim storage in the waste tanks there have been instances of corrosion failures of the waste tanks and their associated equipment. These failures have been used to improve the facilities and ensure that the tanks are viable until the completion of the mission. This paper reviews the corrosion failures that occurred and the actions that were taken to mitigate corrosion to ensure that the risk of tank failure was minimized.

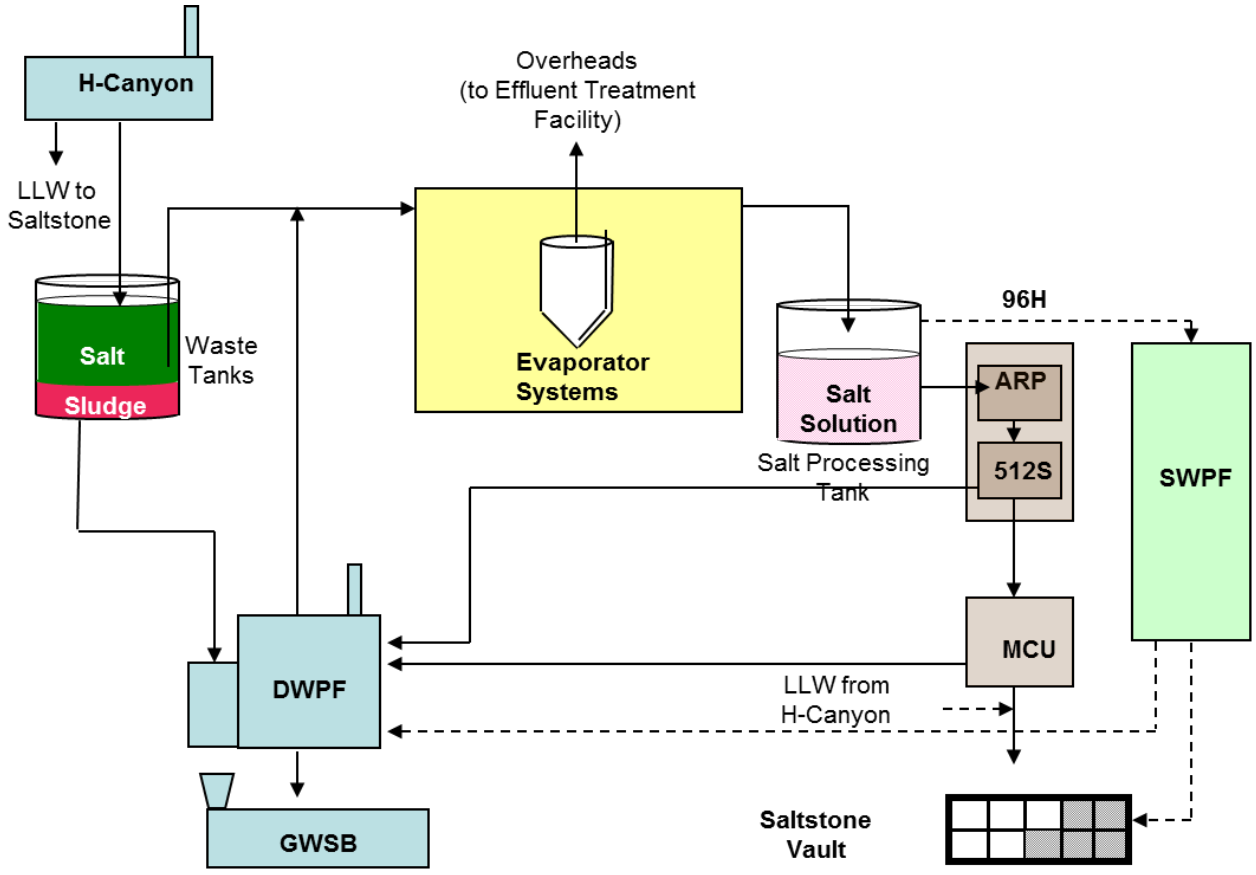

Figure 2. SRS Waste Storage and Processing.

Waste Tank Design and Materials

The steel tanks and liners of the SRS waste tanks were designed and fabricated in accordance with several editions of Section VIII, Division 1 of the American Society of Mechanical Engineers (ASME) Boiler and Pressure Vessel Code (BPVC) [1], depending on the vintage and type of tank, as listed in Table 1 below. Details of the design and materials of construction for the four different types of tanks are described below.

Table 1. Summary of Savannah River Waste Tank (Steel) Design Codes

Tank No.	Type	Year Built	Material of Construction for Primary Tank	Steel Design Code
1F - 8F	I	1952	A285 Grade B	ASME BPV- 1949
9H - 12H	I	1953	A285 Grade B	ASME BPV- 1949
13H - 16H	II	1956	A285 Grade B	ASME BPV- 1952
17F - 20F	IV	1958	A285 Grade B	ASME BPV- 1956
21H-24H		1962	A212-57T Grade B	
25F-28F	III	1975-78	A516 Grade 70 (N)	ASME BPV- 1956 or 1965 as appropriate
29H - 32H		1967-70	A516 Grade 70	
33F - 34F		1969-72	A516 Grade 70	
35H - 37H		1974-77	A516 Grade 70 (N)	
38H-43H		1976-80	A537 Class I (N)	
44F-47F		1977-80	A537 Class I (N)	
48H-51H		1978-81	A537 Class I (N)	

(N) - Normalized

Type I Waste Tanks

The original 12 storage tanks were constructed between 1951 and 1953 and include tanks 1F through 8F in F-Area and 9H through 12H in H-Area. Figure 3 is a schematic drawing showing the dimensions of a Type I tank. Each tank is 75 feet in diameter and 24.5 feet in height and can contain up to 750,000 gallons [2]. The primary tank is a closed cylinder with a flat top and bottom constructed of 1/2 inch thick A285 carbon steel. The top and bottom are joined to the side wall by curved knuckle plates. The annulus pan is 5 feet deep and 5 feet larger in diameter than the tank. The annulus pan is constructed

of 1/2 inch thick A285 carbon steel.

The carbon steel material for both Type I tanks was formed per specification ASTM A285-50T, Grade B firebox quality (A285). The nominal composition and mechanical properties are shown in Table 2 and 3 [3]. The material is also designated as being of firebox quality, semi-killed, and suitable for arc welding. These designations and grades classify the material as "intermediate tensile strength suitable for stationary boilers and other pressure vessels". The basis for choosing this material was its good ductility and suitable weldability. The plates were not heat treated or stress-relieved to reduce the residual stresses in the weld heat affected zones.

Table 2. ASTM Specified Nominal Compositions for Waste Tank Materials (wt. %)[a]

Material	C	Mn	P	S	Si	Cu	Ni	Cr	Mo
A285 Gr B	0.22	0.80	0.035	0.04	-	-	-	-	-
A212 Gr B	0.31	0.90	0.035	0.04	0.15-0.30	-	-	-	-
A516 Gr 70	0.28	0.85-1.2	0.035	0.04	0.15-0.30	-	-	-	-
A537 Class I	0.24	0.7-1.35	0.035	0.04	0.15-0.50	0.35	0.25	0.25	0.08
A53	0.3	1.2	0.05	0.06	-	-	-	-	-
A106	0.3	0.29-1.06	0.048	0.058	0.1	-	-	-	-

a - Single values denote maximum concentration except for silicon in which case it is a minimum value.

Table 3. ASTM Specified Nominal Tensile Strength, Yield Strength, and Elongation for Waste Tank Materials

Material	Tensile Strength (ksi)	Yield Strength, min. (ksi)	Elongation in 8 in., min., percent
A285 Gr B	50-60	27	27
A212 Gr B	70-85	38	19
A516 Gr 70	70-85	38	17
A537 Class I	70-90	50	22
A53	60 (min.)	35 (min.)	longitudinal - 23.5[a]
A106	60 (min.)	35 (min.)	longitudinal - 23.5[a] transverse - 11.5

a - Tension specimens were 1.5 inches long and the elongation was in 2 inches rather than 8 inches.

The tank is surrounded by a concrete vault. The tank and pan are set on a 30 inch thick base slab and are enclosed by a cylindrical 22 inch thick reinforced concrete wall and a flat 22 inch thick concrete roof. There are twelve 2 foot diameter concrete columns within the primary tank to support the roof. Each column has a flared capital and is encased in 1/2 inch thick A285 carbon steel plate. Furthermore, these tanks are buried beneath approximately 8-9 feet of backfilled soil.

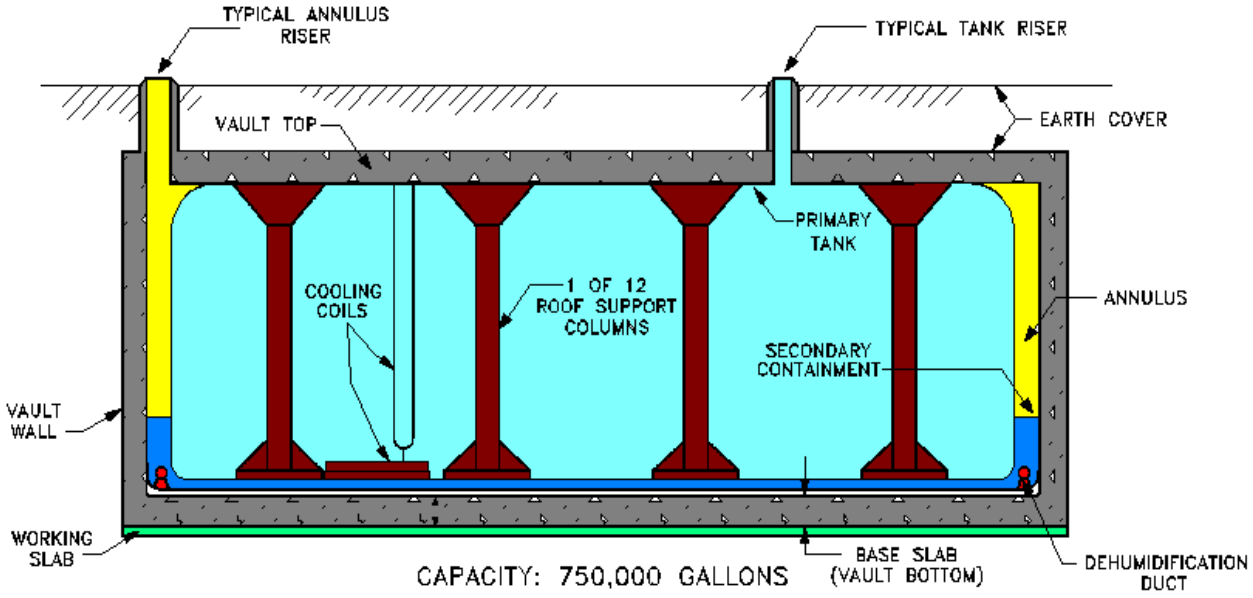

Figure 3. Type I waste tank design.

Type II Waste Tanks

Tanks 13H-16H were constructed between 1955 and 56 and are referred to as Type II tanks. Figure 4 is a schematic drawing showing the dimensions of a Type II tank. Each primary tank is 85 feet in diameter and 27 feet high with a capacity of 1,030,000 gallons [2]. The primary consists of two concentric steel cylinders assembled with a flat bottom and a flat top to form a torus shape. The top and bottom are joined to the outer cylinder by rings of curved knuckle plate. The inner cylinder is joined to the top with a continuous butt weld, and to a base fastened to the bottom with a continuous T-weld. The thickness of the steel plate used for the primary vary depending on location. Plates for the top and bottom were 1/2 inch thick. The knuckle connecting the top to the outer cylinder is 9/16 inch thick, while the knuckle connecting the bottom to the outer cylinder is 7/8 inch thick. The walls of both cylinders are 5/8 inch thick. The primary tank is set in a circular secondary pan which is 90 feet in diameter and 5 feet high. The steel pan is made of 1/2 inch thick steel plate.

These tanks are also surrounded by a concrete vault. The tank and pan assembly is set on a concrete foundation slab that is 42 inches thick. The primary is enclosed by a cylindrical reinforced concrete wall that is 33 inches thick and a flat concrete roof that is 45 inches thick. The roof is supported by the walls and a central concrete column nestled within the inner cylinder of the vessel. The roof of these tanks, however, is at grade level.

The primary tank and the secondary pan were also fabricated from ASTM A285, Grade B carbon steel plate. The plates were not shop heat treated or stress-relieved to reduce the residual stresses in the weld heat affected zones.

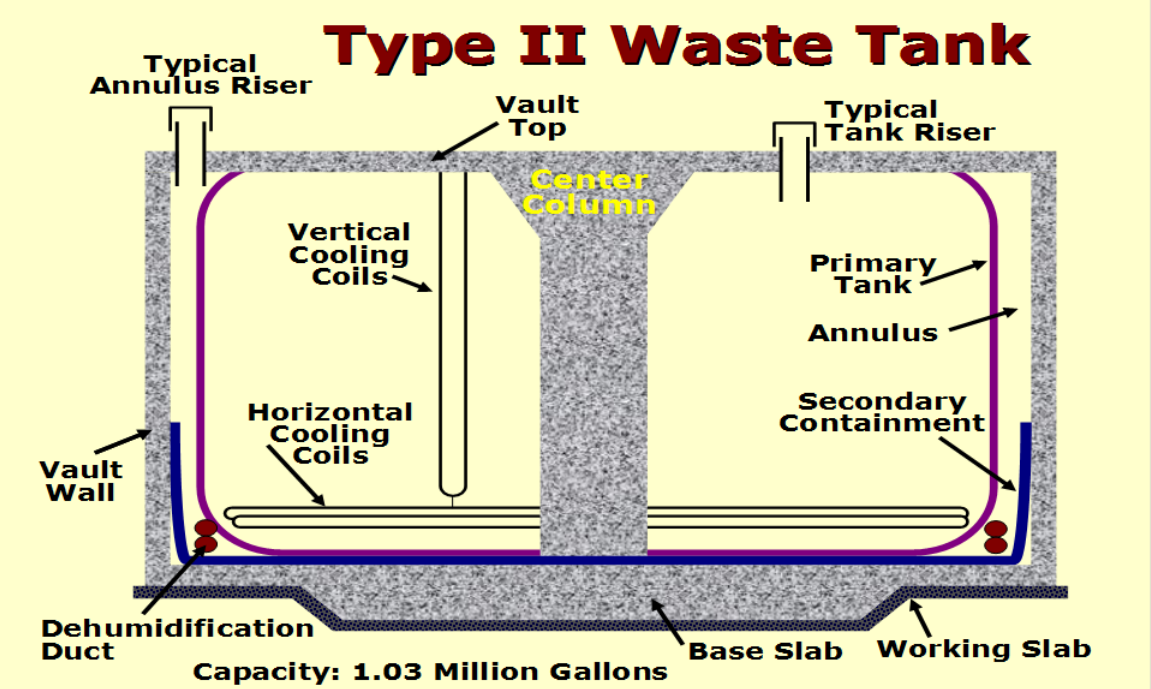

Figure 4. Type II Waste Tank Design

Type III Waste Tanks

The most recently constructed double shell tanks are designated as Type III tanks. The Type III tanks were constructed under seven different projects. Twenty-seven Type III tanks were constructed between 1967-1981 in both F and H areas. Figure 5 shows a cross-sectional drawing of a Type III tank. Each tank is 85 feet in diameter and 33 feet high with a capacity of 1,300,000 gallons [2]. Type III tanks have a toroidal shape similar to the Type II design. Each primary vessel is made of two concentric cylinders joined to washer-shaped top and bottom plates by curved knuckle plates. The plates used to form the primary were of varying thicknesses and are summarized in Table 4. The secondary vessel is 90 feet in diameter and 33 feet high (i.e., the full height of the primary tank) and is made of 3/8 inch thick steel.

The primary tank rests on a six inch bed of refractory concrete. Beneath the refractory is a 42 inch thick concrete foundation slab. The cylindrical walls of the secondary are enclosed by a 30 inch thick reinforced concrete wall and a 48 inch thick flat reinforced concrete roof. Typically there is three inches of cover above the reinforcement steel. A central concrete column fits within the inner cylinder of the vessel. The roof of these tanks is also at grade level.

Table 4. Steel Plate Thicknesses in Type III Tanks.

Plate	Thickness, in.
Top and Bottom	1/2
Upper Knuckle	1/2
Outer cylinder wall	
Upper band	1/2
Middle band	5/8
Lower band	3/4
Inner cylinder wall	
Upper band	1/2
Lower band	5/8
Lower knuckle	
Outer cylinder	7/8 (Tanks 25-28 and 33-51)
	1 (Tanks 29-32)
Inner cylinder	5/8

For Tanks 29-32H both the primary and secondary steel tank are open hearth carbon steel designated as ASTM A516, Grade 70 (A516), fully-killed, and suitable for arc welding. The nominal composition, yield and tensile strengths, and elongation for A537 are shown in Tables 2 and 3. The designation A516 indicates that the steel was made to a fine-grain practice. The fine-grain steel is intended for a lower-temperature service and is tougher, more ductile and undergoes less distortion during heat treatment compared with coarser-grain steels. The plates were not shop heat treated, however, the tanks were stress relieved in the field to reduce the residual stresses in the weld heat affected zones. Tanks 33F and 34F were constructed between 1969-72 from the same material and according to the same code. However, in order to remove the stresses induced by cold forming and to restore dimensional stability, the cold formed knuckle sections of these tanks were shop stress relieved.

The primary tank wall for Tanks 35-37H was fabricated from ASTM A516, Grade 70 normalized (A516N) carbon steel), while the secondary wall was constructed of A516. The nominal composition, yield and tensile strengths, and elongation for A537 are shown in Tables 2 and 3. Both steels were fully-killed,

suitable for arc-welding, and made according to a fine-grain practice. The cold formed knuckle sections of the tank were shop stress relieved, and the tanks were field stress relieved once they were erected. Tanks 25-28F were constructed between 1975-78 from the same materials.

The primary tank for Tanks 38-43H, 44-47F (1977-80) and Tanks 48-51 (1978-81) were all was fabricated of ASTM A537, Class I carbon steel (A537), while the secondary wall was constructed of A516. Both steels were fully-killed, suitable for arc-welding, and made according to a fine grain practice. The nominal composition, yield and tensile strengths, and elongation for A537 are shown in Tables 2 and 3. The A537 steel was selected over the A516N because of its higher yield strength (50 ksi vs. 38 ksi) and lower carbon content (0.24% vs. 0.27%). The higher yield strength ensures that during operations the steel will be at a smaller fraction of its nominal yield stress. The A537 also has a greater fracture toughness than A516 at the tank operating temperatures. The lower NDTT was achieved by the minimization of carbides and the addition of copper, nickel, chromium and molybdenum which provide a more ductile, tougher steel matrix.

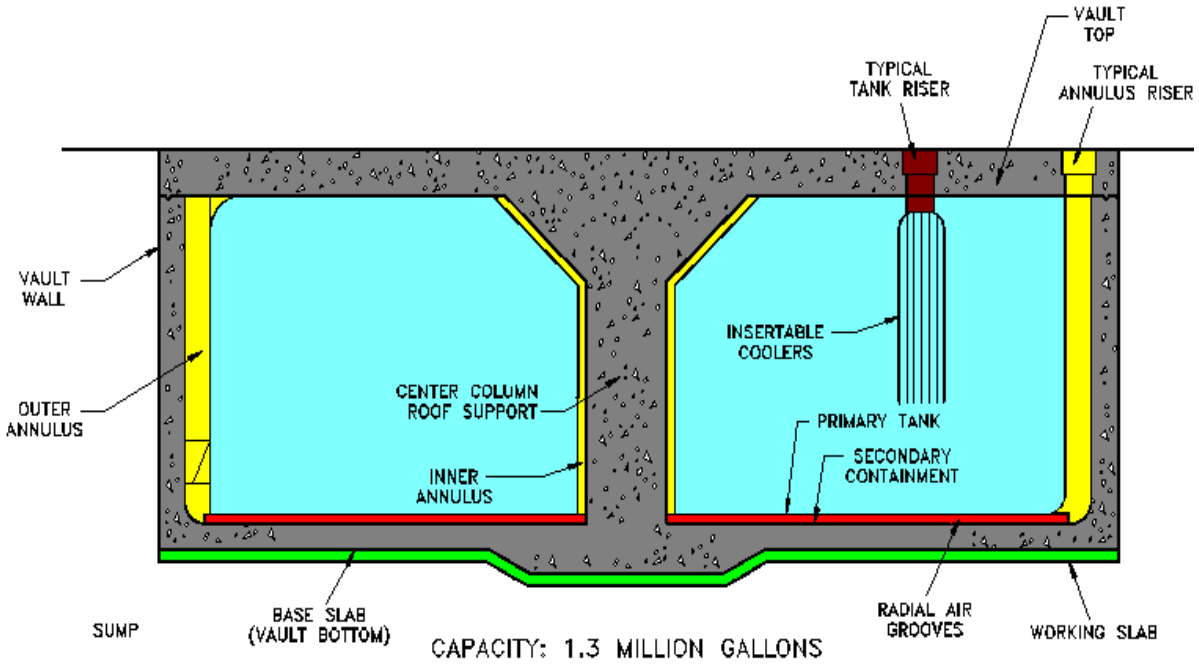

Figure 5. Schematic of Type III Waste Tank

Type IV Waste Tanks

Tank 17F-20F and 21H-24H are single-walled, uncooled tanks and are designated as Type IV tanks. Tanks 17F-20F were constructed in 1958, while Tanks 21H-24H were constructed between 1959-61 [2]. Each tank is 85 feet in diameter and 34 feet high and has a capacity of 1,300,000 gallons. The tanks are

essentially a steel lined, pre-stressed concrete vertical cylinder with a domed roof (see Figure 6). The carbon steel plates used to line the cylindrical walls and the tank bottom were 3/8 inch thick. The knuckle plates at the junction of the bottom and side wall are 7/16 inch thick.

The concrete was built-up around the steel vessel by the "shotcrete" technique, a pneumatic method of application in which a thick, semi-fluid mixture is blown through a nozzle [2]. The wall was pre-stressed by embedding girths of steel under tension in the outer layers of the concrete wall. The concrete dome roof is 7 inches thick, the base is 4 inches thick, and the walls are 13 inches thick. The concrete dome of the tank protrudes above grade level.

A285 was also the material of construction for the liner for the Tanks 17F-20F. The plates were not shop heat treated or stress-relieved to reduce the residual stresses in the weld heat affected zones. Tanks 21-24H were constructed from open hearth ASTM A212, Grade B carbon steel (A212). The material is further designated as firebox quality, fully-killed, and suitable for arc welding. This steel designation and grade classifies it as "high tensile strength suitable for locomotive and stationary boilers and other pressure vessels". This steel was also not shop heat treated or stress-relieved to reduce the residual stresses in the weld heat affected zones. The A212 steel was chosen to replace the A285 because of its higher yield stress, yet still suitable ductility, and greater weldability characteristics.

The nominal compositions, tensile strength, yield strength and elongation for the A285 material is assumed to be the same as for the Type I and II tanks. These values for the A212 material are also shown in Tables 2 and 3. A minimum carbon of 0.18 wt.%, was specified for this material. The minimum carbon content was not required by the ASTM standard, but was included in the site specification for the material. In a commentary on the design of the waste tanks [2] it was noted that, “..a higher minimum carbon content would better resist stress corrosion cracking without field stress relieving.” It should be noted that in 1966 the A212 designation was discontinued and replaced by ASTM A516 (A516-70) [4]. Therefore, A516-70 and A212 are expected to have “comparable chemical and property specifications [4].”

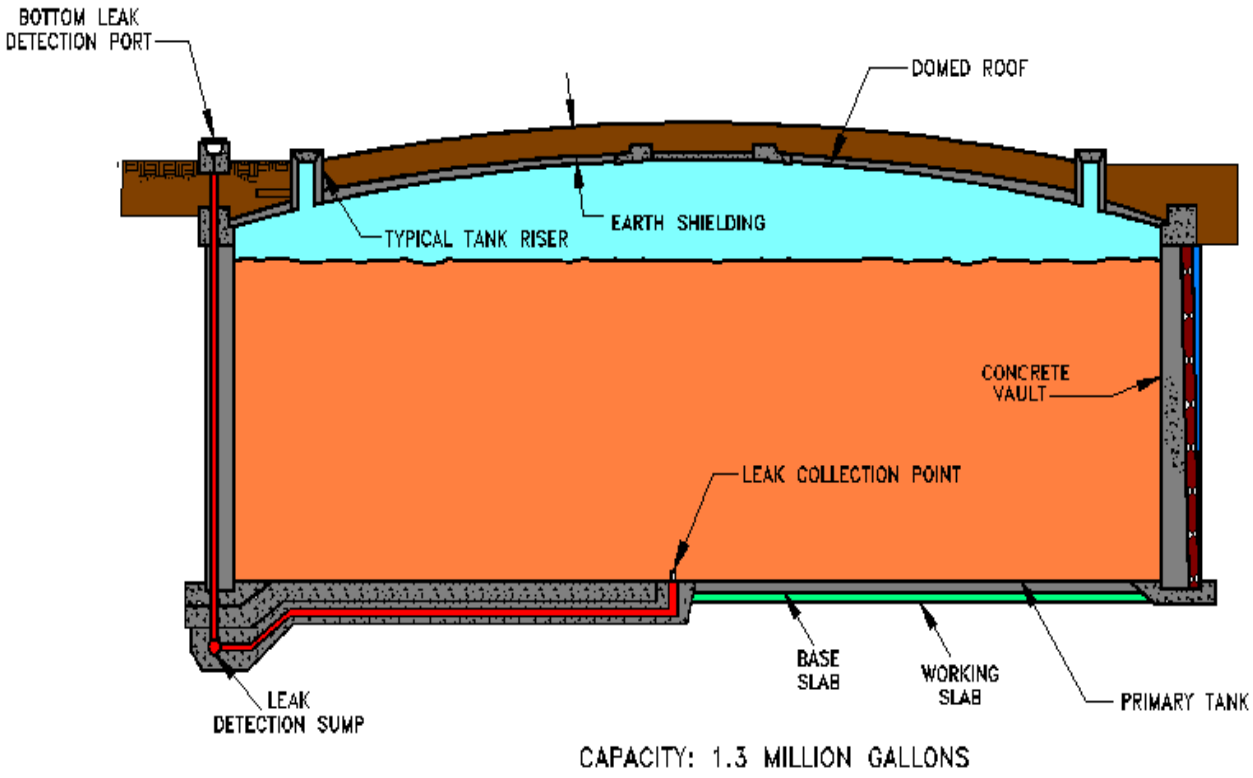

Figure 6. Type IV waste tank design

Waste Tank Cooling Coils

Cooling water that is inhibited with sodium chromate is used to control the temperature of the waste in the tank. There are four types of cooling coil systems installed in the Type I, II, and III tanks. The Type I tanks have 34 vertical pipes uniformly spaced in the tank and two horizontal coils placed near the tank bottom (see Figure 7). The Type II tanks have 40 vertical pipes uniformly dispersed in the tank, two horizontal coils placed near the tank bottom, and two horizontal coils situated in the upper regions of the tank. For Type I and II tanks the vertical coils are supported at the bottom of the tank on four foot triangular centers. The later Type III tanks (25-28 and 36-51) have 23 vertical pipes uniformly distributed throughout the tank. The pipes in these tanks are supported on three foot triangular centers. The earlier Type III tanks (29-35) are cooled by deployable or bundled pipes which are inserted into the tank through risers (see Figure 8). All pipe utilized for the coils, permanent or deployable, is nominally 2 inch diameter Schedule 40 (i.e., 0.154 inch thick).

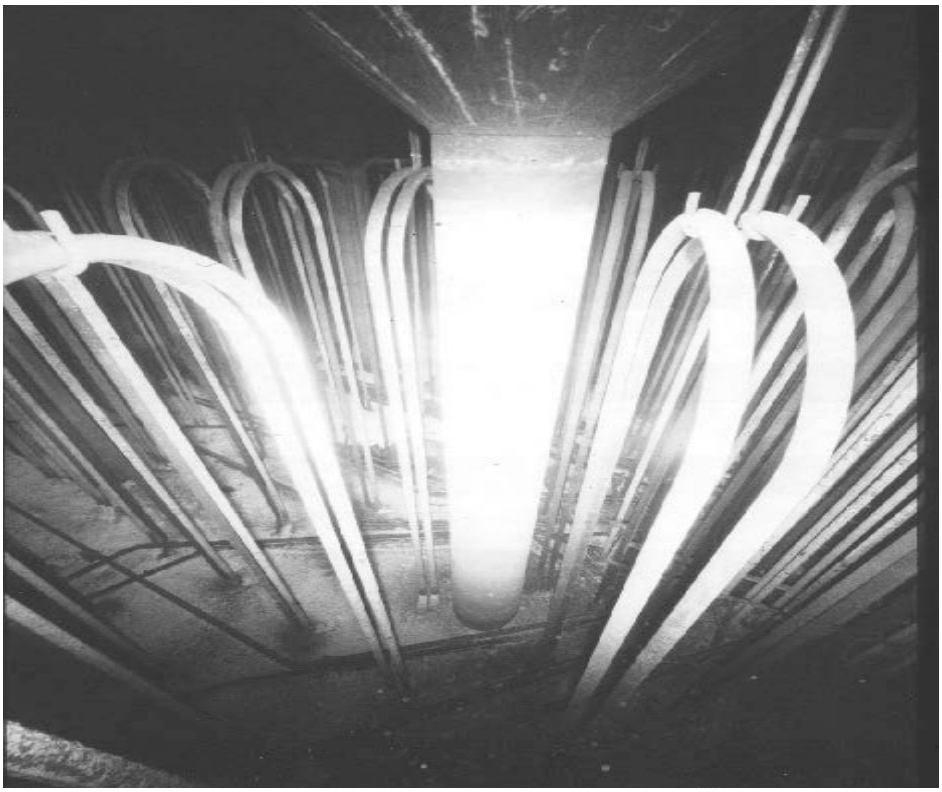

Figure 7. Vertical and horizontal cooling coils in a Type I waste tank. One of the 12 columns is also visible in the photograph.

Figure 8. Deployable cooling coils in an early Type III waste tank. The particular coils are a consolidated bundle style.

The cooling coils are fabricated from either ASTM A53 Grade B or ASTM A106 Grade B seamless carbon steel piping. Seamless pipe is a tubular product made without a welded seam. It is manufactured by hot working steel and, if necessary, subsequently cold-finishing the hot-worked tubular product to produce the desired shape, dimensions, and properties. The nominal compositions and tensile properties for each material are shown in Tables 2 and 3, respectively. The cooling coils in the Type I and II tanks tended to be made of A53, while the coils in the Type III tanks were constructed of A106.

Waste Composition

The waste that is stored in the SRS tanks may be classified into two broad general categories, high heat waste (HHW) and low heat waste (LHW), which are defined by their rate of heat generation. The majority of the HHW are byproducts of the Purex (primary process in the F-Area separations canyon) and the HM or enriched uranium (primary process in the H-Area separations canyon) processes. Wastes from the Purex process are found in both F and H-Area tanks, while wastes from the HM process are stored exclusively in H-Area tanks. A majority of the LHW are also byproducts of these processes. However, other processes and facilities such as resin regeneration, decontamination, and laboratories also contribute significant quantities of LHW.

Both HHW and LHW are present in three forms: supernate, sludge, and salt cake. The supernate is a multicomponent aqueous mixture of sodium salts (see Figure 9). In 1972 an extensive program was initiated to investigate the tank-to-tank variations in the supernate compositions [5]. The ranges of constituent concentrations of the HHW supernate (Tanks 1-15) are shown in Table 5. The samples are divided into H-Area and F-Area to reflect the different separation processes in the two areas. The compositions of the HHW were variable from tank-to-tank. Nitrate is the primary aggressive anion in the supernate while hydroxide and nitrite are the main inhibitors.

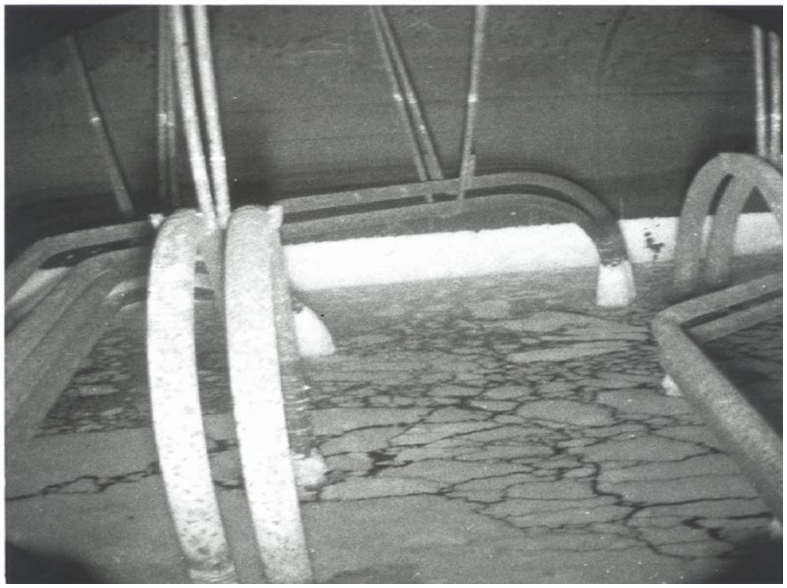

Figure 9. Supernate present in waste tank.

Table 5. Supernate Compositions in SRS High Heat Waste Tanks from 1973-75. Concentrations expressed in moles/liter unless otherwise noted.

Constituent	F-Area	H-Area
Na^+	4.0-12.5	5.7-12.5
NO_3^-	1.6-2.4	1.9-6.4
NO_2^-	0.5-3.1	0.2-3.2
$Al(OH)_4^-$	0.4-0.8	0.4-1.6
OH^-	1.1-6.3	0.8-3.8
$CO_3^=$	<0.1-0.3	<0.1-0.3
$SO_4^=$	0.02-0.18	0.02-0.08

Analysis of LHW was initiated in 1975 [6]. The ranges of constituent concentrations of the LHW supernate (Tanks 17-24) are shown in Table 6. There was also tank-to-tank variability in the LHW compositions. The concentrations of the major constituents (Na^+, NO_3^-, NO_2^-, OH^-, $Al(OH)_4^-$) were higher in the F-Area supernates (Tanks 18-20) because the supernate was in equilibrium with salt. Minimum concentrations in H-Area LHW were low due to Tank 23H which contained water from a fuel storage basin and wastes from regenerating ion exchange columns.

Since the late 1970's, waste from all the tanks has been routinely sampled. Table 7 shows the nitrate, nitrite, and hydroxide concentrations for the different waste types and tank materials. The waste compositions still exhibit variability from tank-to-tank. In general, the composition of the supernates is less corrosive at present than in the past. This change is due primarily to the a) formation of more salt cake which leaves a supernate rich in hydroxide and nitrite and b) the development of chemistry requirements for the supernates in the late 1970's.

Table 6. Supernate Compositions in SRS Low Heat Waste Tanks from 1973-75. Concentrations expressed in moles/liter unless otherwise noted.

Constituent	F-Area	H-Area
Na^+	3.2-11.0	0.2-4.0
NO_3^-	1.9-2.6	0.2-2.8
NO_2^-	<0.05-1.6	<0.05-0.25
$Al(OH)_4^-$	0.1-1.1	<0.01-0.06
OH^-	1.4-7.9	0.06-1.5
$CO_3^=$	0.008-0.05	<0.005-0.02
$SO_4^=$	0.05-0.08	0.005-0.18

Table 7. Supernate Compositions in SRS High Heat Waste Tanks in June 1993. Concentrations expressed in moles/liter.

Waste Type	NO_3^-	NO_2^-	OH^-
F-HHW	1.17-2.96	0.37-3.41	1.08-13.98
H-HHW	1.57-3.19	0.86-2.38	1.02-9.17
H-LHW	0.02-0.18	0.12-0.24	0.28-0.51

Salt cake is formed as evaporated supernate cools in the waste tank (see Figure 10). The solid crystals which form are rich in $NaNO_3$, Na_2CO_3, and Na_2SO_4, while the concentrated supernate is richer in NaOH and $NaAl(OH)_4$. Salt cake contains approximately 78 vol. % salt crystals, which form after the evaporated supernate is cooled, and 22 vol. % interstitial concentrated supernate (i.e., high hydroxide concentration). The composition of the salt varies from tank to tank and is inhomogeneous within a tank. Arithmetic averages of analytical data from samples were used to estimate the saltcake compositions in F- and H-Areas [7, 8]. Table 8 shows the composite salt and concentrated supernate compositions for both of these areas.

Figure 10. Salt cake formation in waste tank and on cooling coils.

Table 8. Composite salt crystal and concentrated supernate compositions in the high level waste tanks.

Constituent	H-Area Salt crystal (wt%)	H-Area Concentrated Supernate (wt%)	F-Area Salt crystal (wt%)	F-Area Concentrated Supernate (wt%)
$NaNO_3$	51.7	42.1	66.4	26.3
$NaNO_2$	11.3	16.9	1.44	24.1
NaOH	2.77	17.8	7.4	30.1
Na_2CO_3	13.4	1.66	4.84	0.33
$NaAl(OH)_4$	5.19	16.7	7.75	14.4
Na_2SO_4	11.5	0.81	9.54	0.35

Table 9 shows a recent sample analyses of saltcake and concentrated supernate taken from Tank 41H. Although there are some differences, the general composition of the saltcake is consistent with the concentrations based on the arithmetic averages.

Table 9. Salt crystal and concentrated supernate compositions in Tank 41H.

Constituent	Salt crystal (wt%)	Concentrated Supernate (wt%)
$NaNO_3$	62	13.0
$NaNO_2$	0.98	6.2
NaOH	3.1	20.6
Na_2CO_3	9.9	3.8
$NaAl(OH)_4$	0.64	2.3
Na_2SO_4	0.50	0.14

The term sludge refers to the gelatinous insoluble layers which settle from the alkaline waste solutions to the bottom of the tank (see Figure 11). The sludge consists of approximately 20 vol. % solids and 80 vol. % supernate [9]. The solids are complex mixtures of more than 30 elements in the form of hydrous oxides. The most prevalent metal oxides in the sludge are iron, manganese, aluminum and uranium. The sludge solids contain about 80 wt. % soluble salts such as $NaNO_3$, $NaNO_2$, NaOH, Na_2SO_4, etc. The majority of the radioactive fission products also remain in the sludge [10].

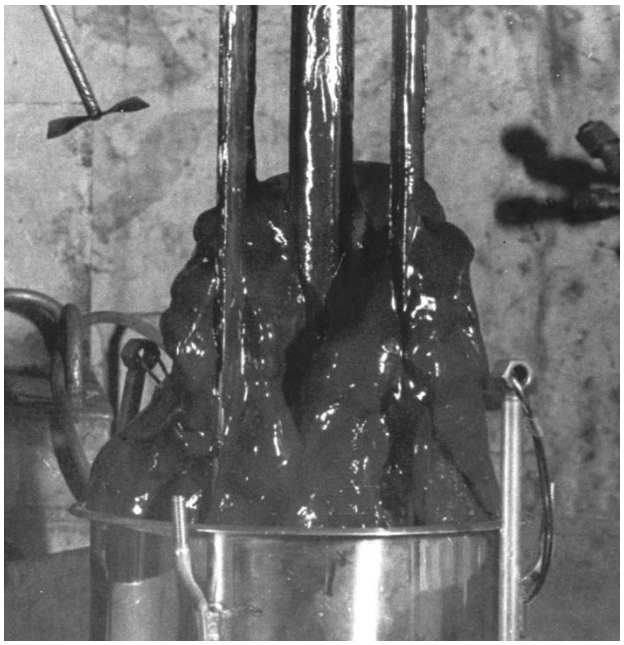

Figure 11. Sludge obtained during sampling of waste tank.

The two major separation processes, Purex and HM, produce sludges with distinct characteristics. For

example, the HM sludge will have a higher aluminum oxide concentration than sludge produced by the Purex sludge. Most tanks contain either Purex or HM sludges, although there are cases in which the two sludges were blended (Tanks 11-16H) [10, 11]. Due to the complex chemical equilibria which exists in the wastes, the composition of the settled sludge will vary widely from tank-to-tank and even within the same tank.

The composition of the supernate associated with the sludge is compared with the supernate sampled near the top of the tank in Table 10. Tank 5F contained sludge from high heat Purex waste. The data show that there is a significant decrease in both the corrosive (nitrate) and the inhibiting anions (nitrite and hydroxide). Fission products present in the sludge convert the nitrate in the sludge supernate to nitrite by radiolysis [12]. Nitrite and hydroxide concentrations are also reduced by radiolysis, however, this occurs at a slower rate. Thus, as the waste ages the nitrate concentration decreases and the nitrite concentration increases. Tank 13H, which contained a 60/40 mixture of HM to Purex sludge, also demonstrated a decrease in the nitrate concentration from the supernate to the sludge. However, the nitrite and hydroxide concentrations were constant or increased slightly. These differences between these compositions and those from Tank 5F may be associated with lower fission product activity in the sludge for Tank 13H. The lower fission product activity would result in less conversion of these anions. Tank 15H sludge consisted primarily of HM sludge and demonstrated the same compositional changes.

Table 10. Comparison of Supernate Compositions with Supernate Associated with Sludge Compositions in Selected Waste Tanks. Concentrations expressed in moles/liter.

Type of Waste	Date Sampled	Temp. (°C)	NO_3^-	NO_2^-	OH^-
Tank 5F Supernate (Purex)	3/1/73	38	2.4	3.1	4.4
Tank 5F Supernate w/ Sludge (6 yr)	10/4/74 - 10/14/74	38	0.44-0.66	0.49-0.78	0.937-1.88
Tank 13H Supernate (Purex and HM)	12/19/72	46	3.6	0.5	1.1
Tank 13H Supernate w/ Sludge (6.5 yr)	8/5/74 - 8/30/74	56	2.15-2.97	0.76-1.0	1.21-1.68
Tank 15H Supernate (HM)	12/19/72	41	3.6	1.1	1.0
Tank 15H Supernate w/ Sludge (3 yr)	10/17/74 - 10/23/74	63	1.77-2.44	0.69-0.91	0.63-1.07

Temperature is an important parameter affecting corrosion response. Due to the fission products in the sludge layer, the temperature in the sludge is generally higher than in any other waste region of the tank. The maximum temperatures in the sludge have historically been between 100-150° C. Unqualified records indicate that the sludge temperatures in some tanks during the early sixties were between 150-

350° C. The higher temperatures would make the steel next to the sludge region more susceptible to corrosion attack. It is difficult to estimate how much of the tank is susceptible to pitting, since the sludge supernate taken from the top of the sludge layer may be significantly different from the sludge supernate in contact with the metal.

Currently, there is approximately 36 million gallons of waste stored in the tanks [13]. The approximate percentage of each phase of waste is shown in Figure 12. The figure also shows the percentage of usable and unusable space in the tanks. The tanks may have unusable space due to leak sites or flammability concerns. The amount of usable space is equivalent to approximately five Type III waste tanks.

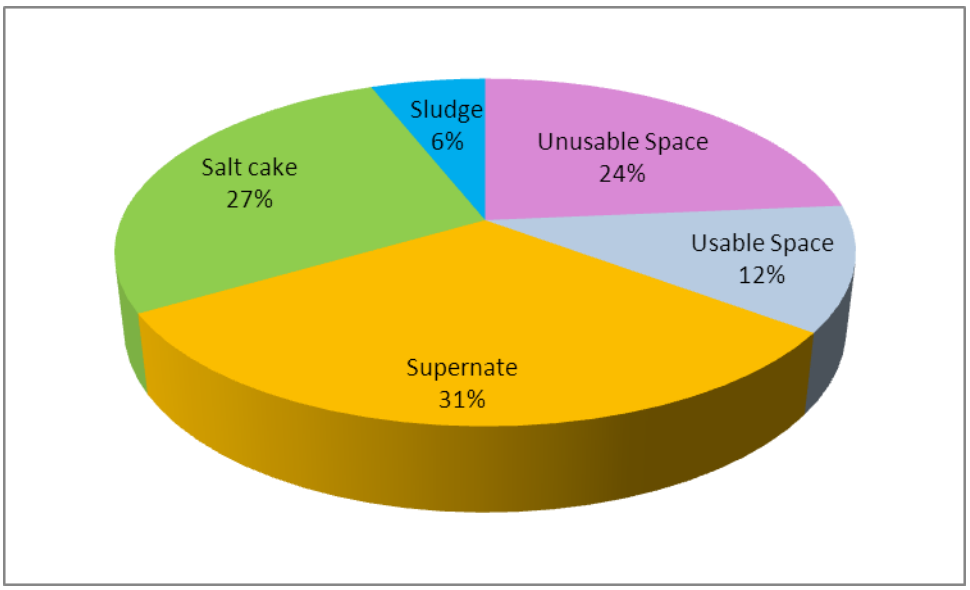

Figure 12. Approximate inventory of waste at SRS as a percentage of total tank volume.

Stress Corrosion Cracking of Waste Tanks

Stress-corrosion cracking has been the principal degradation mechanism for the primary liner in waste storage tanks that have not been stress-relieved. Eight Type I waste tanks and all four Type II waste tanks have developed through-wall leak sites. Leaks developed in tanks 9H, 10H, 14H and 16H within less than two years after being placed in service [14]. The largest leakage of radioactive waste, approximately 185,000 gallons from the primary into the annulus, occurred from Tank 16H, a Type II waste tank. An estimated 700 gallons overflowed the secondary pan in the annulus and therefore impacted the surrounding environment.

Much of what is known with regard to flaws in waste tanks at SRS was learned in conjunction with the leakage incident in Tank 16H, a Type II tank, that occurred in the early 1960s [15]. Data on flaw

characteristics was gathered through visual inspections of the tank, destructive examination of a tank sample and laboratory testing on welded plates. Type I tanks also contain similar flaws, which is not unexpected given that they were constructed of the same materials, were not post-weld heat treated, and were exposed to similar waste chemistry.

Two disks, each 5 5/8 inches in diameter, were extracted from the wall of Tank 16 in 1961 [14]. The disks were extracted from the horizontal weld between the upper knuckle and the upper primary shell plate and both contained leak sites. The steel at this site had been exposed to radioactive waste for approximately 7 months. Metallographic examination revealed three cracks on one of the samples (see Figure 13), with two of the cracks being through-wall. The cracks were intergranular and essentially perpendicular to the horizontal weld (see Figure 14).

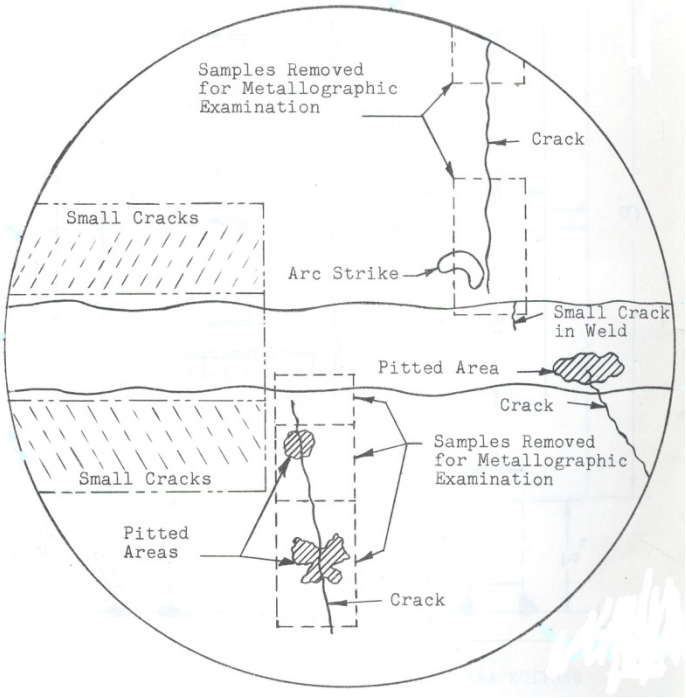

Figure 13. Drawing of interior surface of sample removed from Tank 16H.

Numerous small cracks were observed on the inner surface. These cracks were located in both the knuckle and primary shell plates in bands approximately 0.5 inch wide. The edge of these bands was located between 0.0625 and 0.125 inch from the edge of the weld. The cracks ranged from 0.0625 to 0.5 inch in length and were 0.031 inch deep. Severe stress raisers (e.g., arc strikes, weld beads, weld repairs, etc.) were not required to initiate the cracks, but may have been required to propagate the cracks.

The microstructure of the sample was consistent with the theory that the presence of grain boundary carbides in low carbon steel increases the tendency towards intergranular cracking (see Figure 14). These carbides would be re-dissolved, and hence not present in the weld or immediately adjacent to the weld. This observation would explain why the two major cracks did not propagate into the weld and the numerous surface cracks did not extend into the narrow zone immediately adjacent to the weld.

Shallow pitting occurred at several locations. The pits were broad and approximately 0.02 inch deep at the site of very tightly adherent deposits. Microscopic pits were associated with the intergranular cracks.

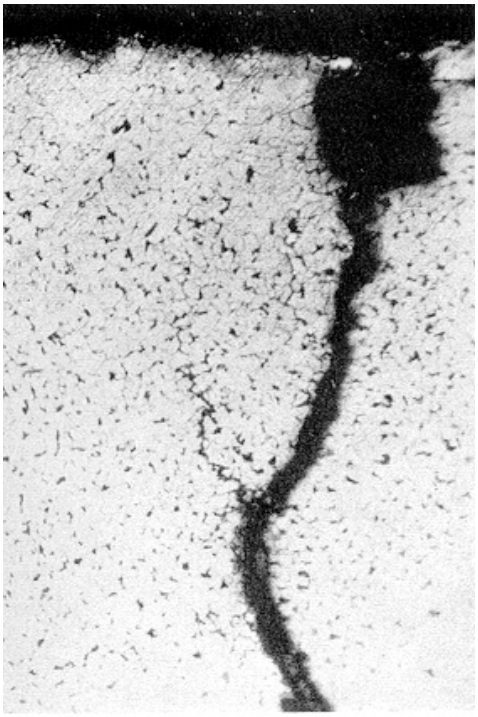

Figure 14. Shallow cracks on interior surface of Tank 16 sample.

Visual inspections were performed on the Tank 16 primary wall shortly after waste leakage was detected [14, 15]. Approximately 73% of the primary wall was inspected during 1961-62 and regions where leak sites were most prominent were identified. The same regions were examined in 1973-74 after the waste had been decanted for the final time. In 1961-1962 approximately 145 leak sites were identified. The leaks were observed on all three horizontal welds, three vertical welds in the upper primary shell, and at several mid-plate sites. Photographs of three leaks at the top horizontal weld were compared with construction radiographs and a correlation between the leaks with weld repairs was established. Two leaks occurred at sites where an alignment plate was attached during construction and the other occurred where extra weld metal was deposited on the interior. The leaks in this tank were fairly well distributed between the three horizontal welds. This result is in contrast to Tank 14, another Type II tank, where all the leaks were located along the bottom horizontal weld. A mid-plate leak was sandblasted and examined by periscope and reflectoscope (a type of ultrasonic measurement). The reflectoscope inspection revealed an attachment on the tank wall near the leak site.

In 1973-74, additional inspection ports had been added to the tank. The survey indicated that the wall contained an estimated 350 leak sites. An exact count of the number of leak sites was not feasible due to larger salt deposits obscuring the smaller ones. Salt deposits on the walls at previously observed leak sites were thicker than before, indicating seepage during the period of time between the inspections. The largest salt deposit was observed on a vertical weld in the upper shell primary plate. A second significant salt deposit was observed beneath the middle horizontal weld.

A comparison of the two inspections indicated that new leak sites had formed. The majority of the new leak sites were observed on the bottom horizontal weld. There was only one or two new indications within the 100” zone that had been a vapor space environment for seven years. However, it should be noted that this region was covered with supernate for the final five years prior to decanting the waste. The top weld, where several leak sites were observed in 1961-62, was not exposed to waste. Therefore it was unknown if any new leak sites developed in this region.

The flaw lengths were also determined. In June 1962, the vertical weld in the upper primary shell beneath an inspection port was sandblasted and then inspected with dye penetrant [15]. Ten large cracks were visible without magnification. The cracks were essentially perpendicular to the weld bead (see Figure 15). Four of the cracks were estimated to be between 4 to 6 inches long. The radiograph of the vertical weld and the photographs revealed exterior surface imperfections as well as internal weld beads. Although three of the cracks appeared to be associated with weld beads, most of the cracks showed no correlation with known fabrication blemishes. One crack appeared to be slightly curved, however, this crack was located next to a repair weld at the intersection of the vertical weld and the middle horizontal weld. All of the cracks appeared to be in a 3-inch zone next to the weld and therefore likely affected by fabrication residual stresses. One crack was observed near a repair weld at the intersection of the vertical and horizontal weld. The crack had an arc like appearance (see Figure 16).

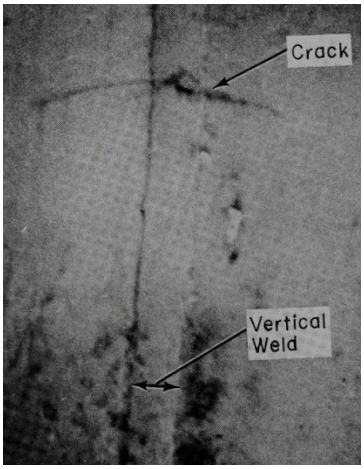

Figure 15. Dye-penetrant testing of stress corrosion crack on vertical weld in Tank 16 [15].

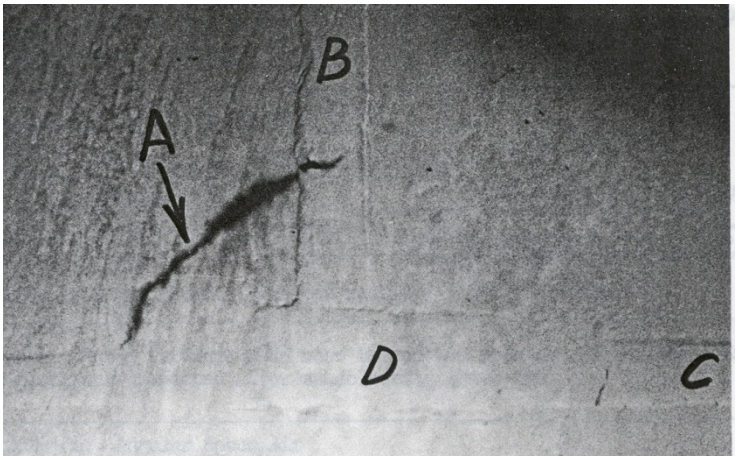

Figure 16. Dye-Penetrant testing at the intersection of vertical and middle horizontal weld in Tank 16: A) crack, B) vertical weld, C) middle horizontal weld, D) repair weld [15].

In January 1974, the same weld was sandblasted and re-inspected with dye penetrant [15]. The cracks did not appear to have increased in size since the 1962 inspection. This result indicated that weld residual stresses were the primary crack driving force.

Since the late 1960's the site has mitigated the risk of leakage from the Type I and II tanks to the environment by maintaining the liquid level below the lowest known leak site in a tank and by removing the waste and storing it in newer waste tanks. The Type III waste tanks were designed and built to mitigate these against these issues. Improved materials of construction as post-weld heat treatment for stress relief were employed for these tanks.

A laboratory corrosion test program was performed to demonstrate the benefits of post-weld heat treatment [14]. Welded test specimens were exposed to a simulated waste solution (5 M nitrate at 97 °C) to induce stress corrosion cracking. Attachment and weld repairs were tested as well as seam welds. The crack patterns that developed around these welds were similar to those observed in the tank.

Figure 17 shows the crack pattern associated with a weld attachment. Weld attachments are typically fillet welds rather than full penetration welds. An arc-like crack that curves through the center of the attachment was observed. It is also interesting to note that the attachment redistributes the residual stresses so that the crack that is roughly perpendicular to the seam weld begins to arc. It was difficult to distinguish whether the crack initiated from the seam or the attachment.

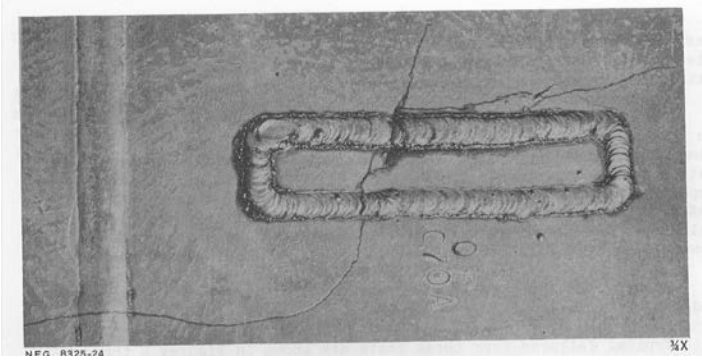

Figure 17. Stress corrosion cracking in area near weld attachment [14].

Figure 18 shows the crack pattern associated with a weld repair. A repair weld is performed to remove defects found in weld beads and the base material during pre-service radiography inspections. During repair, a groove is prepared by grinding out the original weld metal. The repair groove is then filled with new metal. The actual repair length, width and depth may vary depending on the defect size. Cracks

were observed proceeding both through and around a repair weld, although the latter was more frequently observed. Typically the crack traces an arc-like path around the repair and then tends to radiate from the corners.

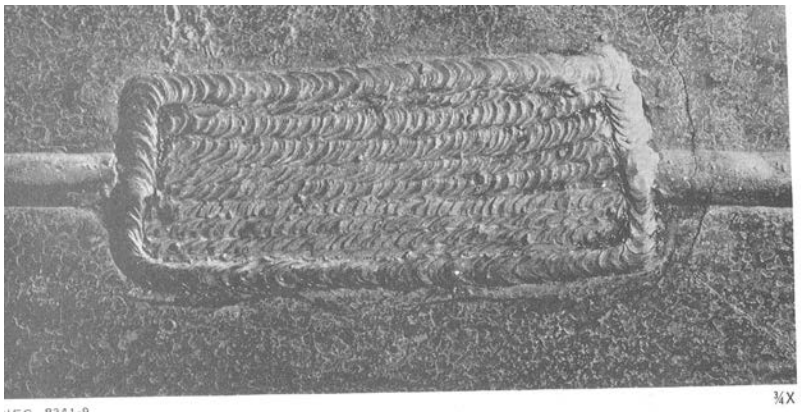

Figure 18. Crack pattern near a weld repair [14].

These tests also showed that a full stress relief of a welded specimen successfully prevented initiation of a stress corrosion crack. The full stress relief procedure was:

1) Place the specimens in the furnace when the furnace temperature is less than 316 °C.
2) Control the heating rate of the furnace such that between 316 to 593 °C, the temperature does not increase at a rate greater than 200 °C/hour.
3) Maintain the temperature at 593 °C for 30 minutes.
4) Control the cooling rate of the furnace such that between 593 to 316 °C, the temperature does not decrease at a rate greater than 260 °C/hour.

All Type III tanks received a full stress relief for greater than 1 hour at a temperature of greater than or equal to 593 °C.

In addition to the stress-relief, a chemistry control program was developed to mitigate the initiation of new cracks and arrest the growth of existing cracks. The waste solutions contain anions which can both cause or inhibit stress corrosion cracking. Nitrate or hydroxide may initiate SCC, however, the presence of either will inhibit cracking by the other. Nitrite which is present in the waste will also inhibit cracking [16]. Electrochemical polarization studies show that carbon steels are susceptible to nitrate SCC in potential ranges between -0.3 to 1.1 V vs. a saturated calomel electrode, while hydroxide SCC occurs at potentials between -0.8 to -1.0 V [17]. In addition hydroxide SCC only occurs at temperatures in excess of 100 °C, whereas nitrate SCC may occur at lower temperatures [18]. Given that the open-circuit potential measured in several waste tanks is between -0.44 to -0.064 V [19] and the temperature of the waste is generally less than 100 °C, the observed cracking is believed to have been caused by the nitrate.

Controls on the solution chemistry were instituted in the late 1970's to preclude the initiation and propagation of SCC for A285 carbon steel. The control limits for supernate with a high nitrate concentration (i.e., greater than 1 M were based on the results of 1) Impressed current and impressed potential slow strain rate tests, which emphasize the conditions for crack initiation [20] and 2) Modified wedge opening loaded (WOL) specimens with a fatigue pre-crack, which evaluate conditions that cause crack propagation [19]. The tests evaluated the effect of nitrate concentration, hydroxide and nitrite concentrations, and temperature on the susceptibility of carbon steel to SCC. Data from both methods is shown in Figure 19. Good agreement existed for the two approaches in that compositions that cause cracks to form also cause them to grow. The figure also shows the recommended limits for the supernate for nitrate concentrations between 3 and 5.5 M. The supernate chemistry limits that were implemented for the tanks in 1977 are shown in Table 11. These are also the supernate chemistry limits that were adopted for the Hanford waste tanks in the 1980's.

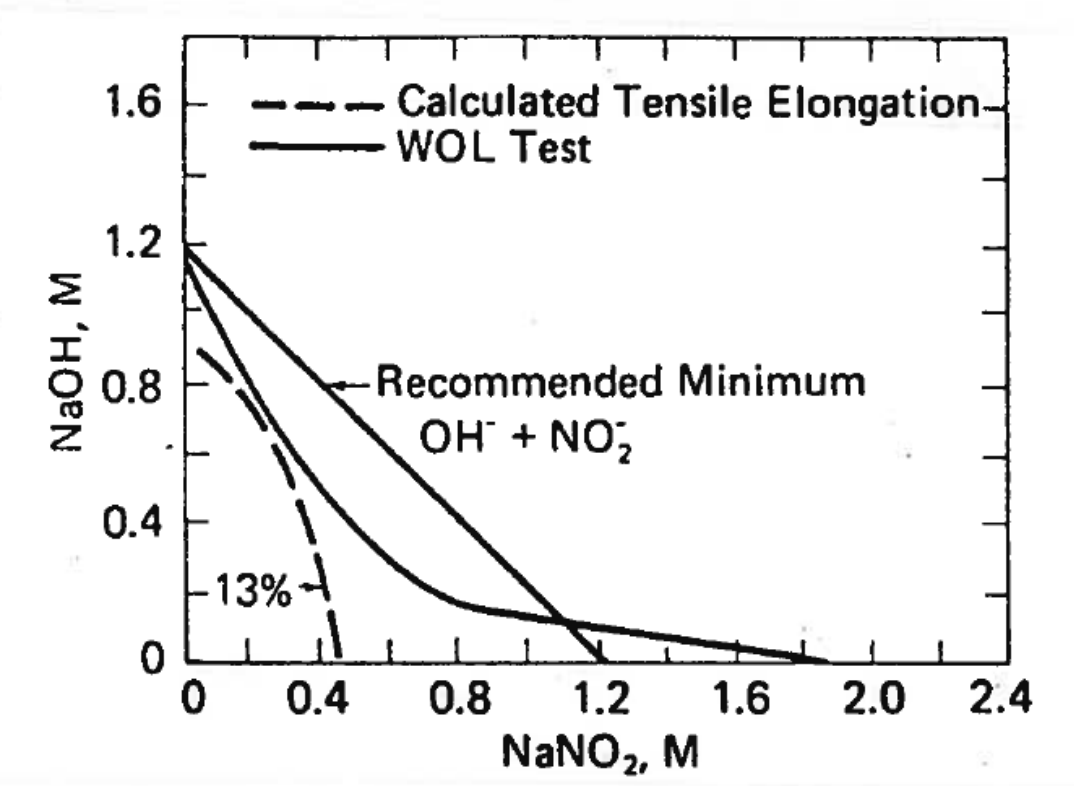

Figure 19. Comparison of WOL and Strain Rate Test Results.

Table 11. Corrosion Control Limits for Supernate

	Minimum	Maximum
NO_3^- in the supernate, M	-	5.5
For NO_3^- between 3.0 to 5.5 M		
OH^-, M	0.3	-
OH^- + NO_2^-, M	1.2	-
For NO_3^- between 1.0 to 3.0 M		
OH^-, M	0.1 * [NO_3^-]	-
OH^- + NO_2^-, M	0.4 * [NO_3^-]	-
For NO3- 3.0 to 5.5 M		
OH^-, M	0.01 (pH =12)	-

In the early 1980's, the facility performed salt removal operations in the Type I waste tanks. In the process of dissolving the salt cake, samples of the dissolved salt solutions indicated that the nitrate concentrations were greater than the maximum nitrate shown in Table 11. In the 1983, controlled potential slow strain rate tests and WOL tests on A285 were utilized to extend the maximum nitrate concentration from 5.5 to 8.5 M [21]. The tests were performed at temperatures between 35° C - 75° C. The nitrite concentration ranged between 0 - 0.5 M, while the hydroxide concentration ranged between 0 - 1.0 M. The probability of crack propagation and the probability of crack initiation were modeled from these experiments. Crack propagation depended on the nitrite and hydroxide concentrations and was independent of temperature and nitrate concentration within these variable ranges. In general, if the hydroxide concentration was greater than 0.6 M and the combination of hydroxide and nitrite concentration was greater than 1.1 M, cracks did not propagate [21]. The probability of crack initiation on the other hand was dependent on all four variables. Inhibitor requirements increased as the nitrate concentration and temperature increased. At the inhibitor requirements obtained for crack propagation prevention, there may be a low probability of crack initiation if the material is at the yield stress and if the nitrate, nitrite and hydroxide concentrations and temperature are all in the correct combination. However, in the unlikely event cracks initiated at these conditions, their estimated crack length would be 0.001 inches. Cracks of this length were not expected to propagate due to the inhibitors present [22]. Therefore, the limits determined by the condition of zero probability of crack propagation were utilized to modify the chemistry limits shown in Table 11 [23].

Testing of the materials utilized for the Type III tanks (A516 and A537) was also conducted. Although neither of these steels is completely immune to nitrate stress corrosion cracking, the tests indicated that they are more resistant than A285. Impressed current slow strain rate tests in the waste simulants at 100° C showed that A516 was generally superior to A285 in resisting stress corrosion cracking [20]. WOL testing showed that A516 and A537 had similar resistance to crack growth [24, 25].

Stress Corrosion Cracking in the Vapor Space of the Type I and II Waste Tanks

The initial interest in the vapor space corrosion phenomenon was spurred by the appearance of an

apparent stress corrosion crack in the vapor space of Tank 15H, a Type II waste tank. A series of inspection photographs of Tank 15H (Figure 20) showed that the vertical part of the crack exceeded 1.5 inches and the parallel part exceeded 7.5 inches. This crack may have reached its stationary configuration, as there was no crack growth observed from 1996-2000. This observation qualitatively agrees with the theoretical prediction of no crack growth. The visual re-inspection of Tank 15 in 2000 confirmed the existence of the defect. Ultrasonic inspections in 2002 and 2007 confirmed that a through-wall crack existed. A small amount of crack growth, although still within a region impacted by the weld residual stresses.

Figure 20. Suspected Tank 15 Stress Corrosion Crack Growth

The Tank 15H stress corrosion crack was an unexpected phenomenon due to two reasons: (1) apparent growth of the stress corrosion crack while this region of the tank was not exposed to the bulk solution stored, and (2) an atypical curved length of 15 inches. The stress corrosion crack reference flaw size was previously accepted to be 6 inches in length. Stress corrosion cracking found in the non-stress relieved Type I/II tanks is typically limited to the residual stress fields surrounding fabrication welds. The discovery of new leak sites in the vapor space region of Tanks 5H and 6H, which are two Type I tanks, during refill in January 2000 added another driver to determine stress corrosion cracking parameters in the vapor space.

A “zero-step” to the comprehensive technology development roadmap was implemented to determine the impact of vapor corrosion on the structural stability of the tanks. The zero-step consisted of experimentation and a review of the operational experience. The review involved inspection data and operational parameters with respect to vapor space corrosion. The experimentation attempted to determine the corrosion mechanisms that have the greatest influence within the vapor space.

General or localized corrosion may occur in the vapor space due to conditions created by relative humidity and the ability of deposited aggressive species on the tank wall to adsorb humidity to form

localized aggressive solutions [26]. Several mechanisms were proposed for the deposition of aggressive species on the tank wall within the vapor space to include: 1) salt residue on the steel tank left by evaporation or supernate transfers 2) species may have been deposited on the tank wall by evaporation from the supernate, transport as an aerosol followed by condensation on the tank wall. In sufficiently humid conditions, the residue can adsorb atmospheric moisture and dissolve, forming a corrosive electrolyte.

A review of the relevant parameters from operational experience of Type I tanks was performed. The data reviewed included the temperatures, waste levels, and chemistry data, for possible with correlation inspection data collected from ultrasonic testing. The data was analyzed for relevance to vapor space corrosion. The review confirmed that general corrosion in the vapor space is not an unusually aggressive phenomenon and correlates well with predicted corrosion rates for steel exposed to bulk solution. The corrosion rates are seen to decrease with time as expected. Although the data suggest that general corrosion rates at the top knuckle weld of the Type I tanks may be the highest, this may be due to the lack of data points for accurate averaging, and the proximity of the measurement to the thinner edges of the plates. The review of the temperature data did not reveal any obvious correlations between high temperatures and the occurrences of leaks. The complexity of temperature-humidity interaction, particularly with respect to vapor corrosion requires further understanding to infer any correlation. The review of the waste level data also did not reveal any obvious correlations. The review confirmed that general corrosion was not of concern, however, did not address the possibility of localized corrosion mechanisms [27].

The focus of the experimental program was on understanding VS and LAI pitting particularly for application to the Type III HLW tanks. Pitting, rather than stress corrosion cracking, is the primary concern for the Type III tanks, since the risk of SCC has been significantly reduced in these tanks through post-weld heat treatment to relieve residual stresses from fabrication welding.

Experiments performed in FY02 determined the potential for vapor space and liquid/air interface corrosion of ASTM A285-Grade B and ASTM A537-Cl.1 steels. The material surface characteristics, i.e. mill-scale, polished, were found to play a key role in the pitting response. The experimentation indicated that the potential for limited vapor space and liquid/air interface pitting exists at 1.5M nitrate solution when using chemistry controls designed to prevent stress corrosion cracking. The tests were performed at the minimum inhibitor requirements established for this nitrate concentration (see Table 11).

Experiments performed in 2003 quantified pitting rates as a function of material surface characteristics, including mill-scale and defects within the mill-scale [28]. Testing was performed on ASTM A537-Cl.1 (normalized) steel, the material of construction of the Type III HLW tanks. The pitting rates were approximately 3 mpy for exposure above inhibited solutions, as calculated from the limited exposure times. This translates to a penetration time of 166 years for a 0.5-in tank wall provided that the pitting rate remains constant and the bulk solution chemistry is maintained at the minimum inhibitor requirements.

In 2004, testing consisted of electrochemical testing to potentially lend insight into the surface chemistry and further understand the corrosion mechanism in the vapor space. The cyclic polarization testing confirmed that pitting is electrochemically improbable in the vapor space provided the bulk solution chemistry is sufficiently inhibited, for a bulk solution temperature of 50°C [29].

In 2005, testing focused on the effect of the minor waste constituents on the corrosion response of the tank steel [30]. The testing suggested that decanting and the consequent residual species on the tank wall is the predominant source of surface chemistry on the tank wall. The laboratory testing has shown that at the boundary conditions of the chemistry control program for solutions greater than 1M $NaNO_3$:

- Minor and isolated pitting is possible within crevices in the vapor space of the tanks that contain stagnant dilute solution for an extended period of time, specifically when residues are left on the tank wall during decanting,
- Liquid/air interfacial corrosion is possible in dilute stagnant solutions, particularly with high concentrations of chloride or sulfate

The results of the “zero step” program indicated that the current chemistry control program has been sufficient to prevent consequential VSC/LAIC in the Type III/IIIA tanks. However, the results also indicate vulnerability in the chemistry control program when the nitrate concentration exceeds 1 M.

The following revisions, specifically designed to control against VSC/LAIC, were recommended to the chemistry control program:

- The extension of the minimum hydroxide concentration of 1 M for wastes with nitrate concentration greater than 1 M

- Redefinition of minimum nitrite requirements for wastes with nitrate concentration greater than 1 M;

OR the following when the hydroxide concentration is less than 1 M

- The extension of minimum nitrite requirements as a function of concentrations of chloride and sulfate for wastes with nitrate concentration greater than 1 M.

Option 1 of the recommended changes to the chemistry control is a minimum hydroxide concentration of 1 M and a corresponding minimum of 0.2 M nitrite (see Figure 21). As an alternative, Option 2 requires that where the hydroxide concentration falls below 1 M, there is a minimum nitrite concentration of 0.6 M *and* additional requirements on the minimum nitrite concentration as a function of chloride and sulfate. Minimum inhibitor concentrations are to be calculated using chloride and sulfate concentrations measured prior to the most recent decant.

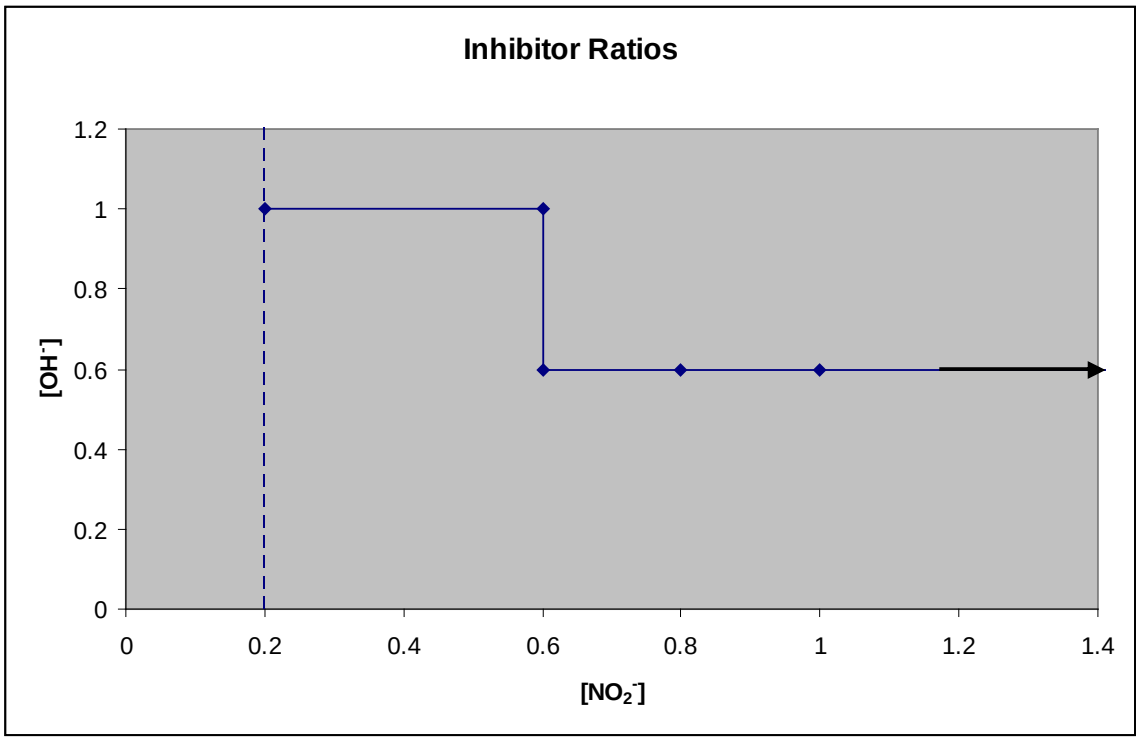

Figure 21. Recommended Option 1 Minimum Hydroxide and Nitrite Requirements

The minimum nitrite concentrations as a function of chloride and sulfate are shown in Figure 22 and Figure 23, respectively. The minimum nitrite concentration limit of 0.6 M is reached at a chloride concentration of 0.012 M. This implies that when the hydroxide concentration falls below 1 M, the minimum nitrite concentration is 0.6 M if the chloride concentration is below 0.012 M. However, the

minimum nitrite concentration is controlled by the chloride concentration when it exceeds 0.012 M. The sulfate concentration for this "cross-over" point is 0.35 M. This implies that when the hydroxide concentration falls below 1 M, the minimum nitrite concentration is 0.6 M if the sulfate concentration is below 0.35 M. However, the minimum nitrite concentration is controlled by the sulfate concentration when it exceeds 0.35 M. If both the concentration of chloride and sulfate exceed the "cross-over" point, the chloride limit is far more restrictive and will control the minimum nitrite required.

Testing indicated that supernate transfers and the consequent residual species on the tank wall is the predominant source of surface chemistry on the tank wall. As such the extent to which the initial solution is inhibited prior to transferring of the solution plays a key role in the corrosion in the vapor space. At the boundary conditions for Chemistry Limits 1 through 3 of the Corrosion Control Program minor and isolated pitting is possible within crevices in the vapor space of the tanks that contain stagnant dilute solution for an extended period of time, specifically when residues are left on the tank wall during supernate transfers.

Table 12 provides supernate chemistry control limits for a tank that is inactive for more than six months [31]. If the tank is active during the six month period, the normal limits remain applicable. These limits apply only to Type III/IIIA tanks. Compliance with these limits will be accomplished by quarterly engineering evaluations to identify any tanks that may not be compliant with the vapor space criteria.

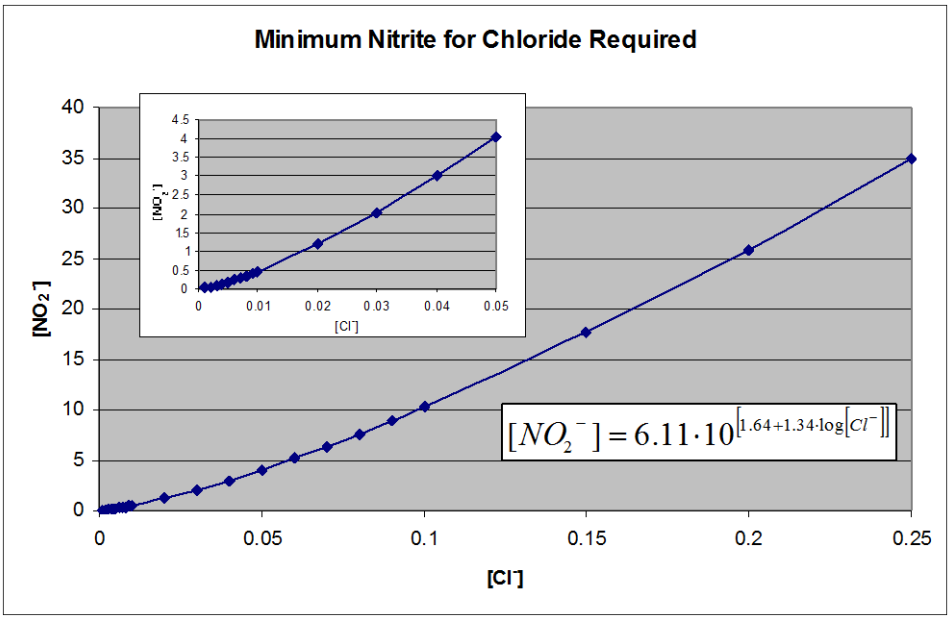

Figure 22. Minimum Nitrite Concentration as Function of Chloride Concentration

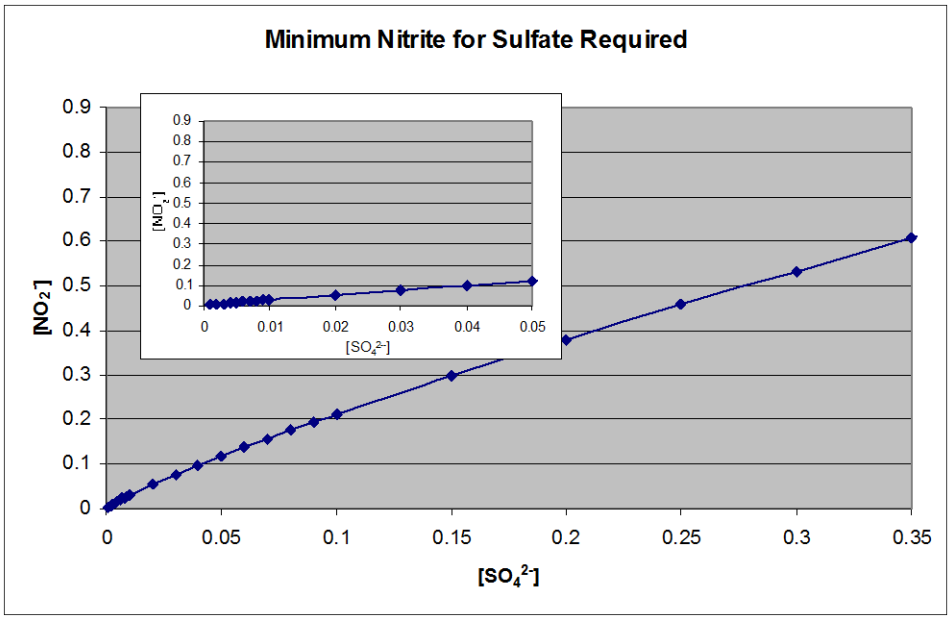

Figure 23. Minimum Nitrite Concentration as a Function of Sulfate Concentration

Table 12 – Minimum Chemistry Requirements for Tanks That Have Been Inactive for More than Six Months

Applicability	Parameter	Minimum Needed (M)
$1 < [NO_3^-] \leq 8.5$	$[OH^-]$	1
	AND $[NO_2^-]$	0.2
	OR	
	$[OH^-]$	0.6
	AND $[NO_2^-]$	0.6
	AND $[NO_2^-]$	$6.11*10^{(1.64+1.34*Log([Cl-])}$
	AND $[NO_2^-]$	$0.04*10^{[1.64+0.84*Log([SO4-])]}$

Pre-service Pitting of Waste Tank Bottom and Waste Annulus

Pits as deep as 0.169 inches were observed on the primary liner bottom during the construction of Tanks 38-51H. An extensive program was performed to determine the cause of pitting, the impact of pitting on the integrity of the tanks, and the remedial actions required to correct the problem [32-34].

The pitting mechanism for the primary tank involved oxygen concentration cells that formed in crevices created by the protective plywood placed on the floor of the tanks. Rainwater that intruded through the tank risers saturated the floor beneath the plywood for extended periods of time and produced conditions conducive to corrosion. Although several factors were considered which may have accelerated the corrosion, the most likely factor was the leaching of amino organic phosphate ions from the fire retardant treatment of the plywood.

The integrity of the tanks was not compromised by the pitting. All tanks satisfactorily met the ASME Code criteria for static stresses and low cycle fatigue. The probability of initiation and propagation of stress-corrosion cracks from the existing pits was determined to be virtually nil.

Grit blasting conducted to clean the tank floor (to facilitate inspection) further reduced the likelihood of stress-corrosion cracking by inducing high compressive stresses in the surface layer. Laboratory tests also showed that grit blasting did not make the tank bottom susceptible to galvanic corrosion [33].

Based on these observations, the pits should not affect the functional performance of the tank provided chemistry control is maintained. These tanks have performed satisfactorily since they were placed in-service.

Pitting corrosion was also observed in the annulus of seven of fourteen new Type IIIA waste tanks under construction in F and H Areas [34]. Pitting was limited to the secondary liner floor plates near the lower knuckle weld. Water had entered the annulus during construction and remained in a stagnant puddle on the secondary liner floor. In these neutral water conditions, the weld metal (ASTM E-7018) was anodic to the base metal (ASTM A516 Grade 70 carbon steel), and therefore more prone to corrosion. Ferrous ion produced by the preferential attack at the weld and weld impurities attracted micro-organisms to the weld area. Analysis of the water samples taken from the annulus and nearby wells indicated the presence of sulfate reducing bacteria (SRB). A mound-like tubercle composed of micro-organisms, sediments and corrosion products formed at the weld. Once the tubercle was established, anaerobic conditions were established in the mound. Pitting proceeded by oxygen concentration aided by the action of the SRB. The maximum pit depth measured was 0.085 inches [35]. The typical construction period was on the order of 12-18 months.

The tanks are equipped with a ventilation system that provides warm, dry air to the annulus region. The effect is to evaporate liquid that may intrude into the annulus and limit condensation. Thus, the formation of microbial colonies has been mitigated successfully while the tanks have been in-service.

Pitting of Waste Tank Cooling Coils

Several coils have failed during tank operations [36]. There are some tanks which have lost as much as 25% of their cooling coils. However, the location, defect size, failure mechanism in most cases has not been precisely determined. Coils from five tanks have been removed and examined metallographically for defects. In 1967, a sixteen inch section was removed from the upper horizontal coil [37]. Leaksites were found in this coil (see Figure 24) and were attributed to pitting from the outside. The size of the pit was approximately 1/8 inch in diameter. Some intergranular attack was also observed beneath the scale formed on the outside. Two coil sections were also removed from the valve house of Tank 16 in 1978 [38]. Since the exterior of the coil was exposed only to air, no corrosion was observed on the outside. The inner surfaces indicated only superficial surface corrosion with a few cases of very mild pitting. No wall thinning was observed. In 1991, sections of failed coils in Tanks 38, 40, and 48 were removed from the valve house [39]. Once again, the inner surface exhibited only superficial surface corrosion and no extensive wall thinning.

Ondrejcin investigated trends and mechanisms for cooling coil failures in Type I and II tanks between 1954-74 [37]. During the first 12 years of operation only one tank, Tank 10, experienced an unsatisfactory cooling coil failure frequency. These failures were attributed to a temporary caustic deficiency in the supernate and were corrected by adding NaOH. From 1967-69, sludge removal operations were carried out in seven of the Type I and II tanks (Tanks 1F-3F, 9H-11H, and 14H). The coils began to fail within a month after the sludge removal operations were initiated (pitting rate of ~ 0.15 inches/month). During this time cooling coil failures dramatically increased (~10/tank-year). The failures were attributed to pitting which resulted from exposure to dilute waste that is low in caustic and nitrite inhibitor and relatively high in sulfate dissolved from the sludge. The failures were hypothesized to occur in the creviced regions of the cooling coil supports. After the tanks were restored to normal chemistry (between 1970-74), failures occurred at a decreased rate (~0.067/tank-year). However, this rate was three times greater than the failure rate that had occurred prior to sludge removal (~0.023/tank-year). The higher failure rate after return to normal chemistry was attributed to coils which were damaged during sludge removal, but had not failed until later.

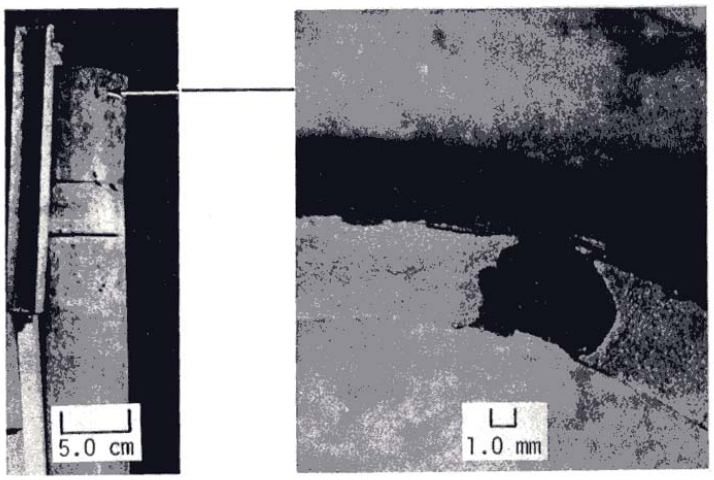

FIGURE 3. Perforated Upper Horizontal Cooling Coil, Tank 2F

Figure 24. Leak site in horizontal cooling coil in a Type I tank.

The cooling coil failures were a result of adding uninhibited water, which diluted the waste, to the tank. Electrochemical tests were conducted to determine the critical concentrations of nitrite and hydroxide necessary to inhibit pitting. The tests showed that water containing 500 ppm nitrite at pH 12 would inhibit pitting in these dilute solutions. This recommendation was used to define a technical basis for inhibition of pitting in dilute waste solutions (see Table 11). These measures should adequately preclude pit initiation by this mechanism. Since these initial requirements, testing was performed to address liquid-air interface corrosion at these limits. Refinements to the limits in Table 11 address the effects of nitrate, chloride and sulfate on pitting at the liquid air interface [23].

More recently, several failures of the cooling coils were discovered in the Type III waste tanks [36]. Over 90% of these failures occurred in three tanks: 38H, 48H, and 50H. The precise location and mechanism by which the recent coil failures occurred has not been determined. Four possible mechanisms have been proposed to explain the failures:

- pitting corrosion of the section of coil in the vapor space region above the waste;
- pitting corrosion in the section of coil embedded in the concrete;
- pitting corrosion due to the depletion of the chromate inhibitor within the coil.
- failures at original defects in the cooling coils.

Attempts to simulate the first three mechanisms in the laboratory were made. Partial immersion coupon tests were conducted to investigate the potential of corrosion in the vapor space above the waste. If the simulant was inhibited properly (i.e., within the corrosion control requirements), no attack

of the coupon was observed in the vapor space. A review of the supernate compositions over the past ten years indicated that the wastes in the Type III tanks had not been outside the technical standard requirements for a significant period of time. Therefore this mechanism seems unlikely. Cyclic polarization tests were performed in on carbon steel immersed in a simulated cement pore water to investigate the potential for chloride induced pitting in the concrete [40]. If the pore water contained approximately 9000 ppm chloride, pitting was induced on the specimen. A sample of concrete taken from the top of a Type III waste tank was analyzed for chlorine. The sample indicated that there was only 10 ppm chloride present in the concrete. This result, coupled with the observation that no staining or spalling of the concrete roof of the tank has been observed [41], indicates that this is an unlikely mechanism.

The third mechanism appears to be a more likely failure mechanism. Normally the well water that is utilized as the cooling medium is inhibited with 400-750 ppm sodium chromate. However, operations frequently places several of the coils within a tank out of service. The result of this action is regions of stagnant water within the coil which may result in depletion of the chromate in localized areas [42]. Cyclic polarization tests were performed with carbon steel immersed in chromate solution at various concentrations. The results showed that the critical concentration of chromate above which carbon steel is not susceptible to pitting is approximately 100 ppm. Depletion rate studies indicate that the chromate concentration may reach this level if the solution remains stagnant for 90-200 days. The lack of a history of cooling coil operations, however, does not allow one to make a direct correlation between the time the coil is out of service and the failure of a coil. As a means of countering this mechanism, since 1992 all coils have been purged with fresh chromate solution every 90 days.

An attempt was made in 1978 to assess the potential for this type of failure mechanism [38]. Tank 16H had experienced 5 cooling coil failures. It was estimated that the cooling water had been stagnant in the coils for seven years. Non-leaking sections of cooling coil pipe were removed and examined for pits on the inside surface. Evidence of localized attack was observed, however, it was considered negligible. However, since the leak sites were not visually examined, this mechanism cannot be ruled out entirely.

The final possibility is that the pipes were installed in the tanks with pinhole defects. Evidence of these defects has been observed during the installation of coils in Tank 38H [43], Tank 43H [44], and Tank 44F [45]. All coils in these tanks had passed hydro-tests prior to being installed. However, visual inspections prior to placing the tanks in-service indicated that the chromate inhibited water was leaking. The coil leak in 38H occurred between the concrete roof and the primary tank liner where the coil penetrates the primary. The failure analysis concluded that dressing by grinding the pipe in a weld region led to the pinhole leak. The coils in Tank 43H and 44F formed at thin spots associated with manufacturing flaws on the outer surface of the coil. The size of the hole and its location in the tank is such that wetness may not have been visible during the hydro-test.

Conclusions

The principle corrosion mechanisms for the waste tanks are localized in nature. The underground carbon steel tanks at the Savannah River Site, in particular the Type I and II waste tanks, have leaked due

to nitrate stress corrosion cracking. However, the presence of a secondary pan has limited the amount of leakage to the environment to an estimated 700 gallons. Improvements to the materials, fabrication methods and waste chemistry control have significantly improved the performance of the Type III waste tanks. These newer tanks have been in service for approximately 40 years with no indications of leakage.

Recently, flaw indications have been observed in the Type I and II waste tanks in the vapor space region above the tanks. The facility continues to monitor the situation. This indication of the possibility of an aggressive condition in the vapor space above the waste has led the facility to investigate vapor space corrosion for the Type III tanks as well. Conditions that may result in aggressive attack are monitored.

Pitting of the primary waste tank wall occurred during construction of some of the Type III tanks, however, it has not been a significant problem during service. However, during operations with dilute solutions, pitting of the cooling coils was observed. Chemistry controls for processes that involve these dilute solutions were recommended.

References

1. Section VIII of the American Society of Mechanical Engineers (ASME) Boiler and Pressure Vessel Code, Years 1949, 1952, 1956, and 1965.
2. B. E. Loper, “Liquid Waste Tank Structural Design Concept”, DPE-3477, June 21, 1977.
3. “Tentative Specification for Low and Intermediate Tensile Strength Carbon Steel Plates of Flange and Firebox Qualities” ASTM A285-52a T, Issued May 1949, Revised, December 1949, September and December 1950, and February and September 1952.
4. G. R. Caskey, “Potential Radiation Damage – Storage Tanks for Liquid Radioactive Waste”, WSRC-TR-92-350, August 1992.
5. R. S. Ondrejcin, "Chemical Compositions of Supernates Stored in SRP High Level Waste Tanks", DP-1347, August 1974.
6. R. S. Ondrejcin, "Composition and Corrosiveness of Low-Activity Waste Supernates Stored at the Savannah River Plant", DP-1427, October 1976.
7. J. R. Fowler, "Composition of F-Area Soluble High-Level Waste", DPST-82-390, March 10, 1982.
8. J. R. Fowler, "Composition of H-Area Soluble High-Level Waste", DPST-82-502, April 28, 1982.
9. D. T. Hobbs, "Supernatant Liquid Sampling in Waste Tanks (U)", WSRC-RP-92-1179, September 23, 1992.
10. J. A. Stone, J. A. Kelley, and T. S. McMillan, "Sampling and analyses of SRP High-Level Waste Sludges", DP-1399, August 1976.
11. J. R. Fowler, "Sludge Composition for Each Tank and DWPF Feed Batches", DPST-84-556, June 11, 1984.
12. M. L. Hyder, "The Radiolysis of Aqueous Nitrate Solutions", **J. Phys. Chem., 69,** 1858 (1965).
13. D. Chew, “September 2013 WCS Curie and Volume Inventory Report”, SRR-LWP-2013-00066, October 2013.
14. M. L. Holzworth, R. M. Girdler, L. P. Costas, and W. C. Rion, “How to Prevent Stress Corrosion Cracking of Radioactive Waste Storage Tanks”, Materials Protection, January 1968, pp. 36-38.

15. W. L. Poe, "Leakage from Waste Tank 16: Amount, Fate, and Impact", DP-1358, November 1974.
16. J. A. Donovan, " Factors Controlling Nitrate Cracking of Mild Steel", in **Proc. Conf. Environmental Degradation of Engineering Materials**, Blacksburg, Virginia, October 1977.
17. R. S. Ondrejcin, "A Stress Corrosion Cracking Test with Slow Strain Rate and Constant Current", Presented at the **ASTM Symposium on Stress Corrosion Cracking**, Toronto, Canada. May 1977.
18. H. Mazille and H. Uhlig, "Effect of Temperature and Some Inhibitors on Stress Corrosion Cracking of Carbon Steels in Nitrate and Alkaline Solutions", **Corrosion 28**, 427 (1972).
19. J. A. Donovan, "Materials Aspects of SRP Waste Storage - Corrosion and Mechanical Failure", DP-1476, November 1977.
20. R. S. Ondrejcin, "Prediction of Stress Corrosion of Carbon Steel by Nuclear Process Liquid Wastes", DP-1478, August 1978.
21. R. S. Ondrejcin, "Salt Removal Compositional Limits - Suggested Technical Standard for Types I, II, and IV Nuclear Waste Tanks", DPST-83-533, July 25, 1983.
22. A. K. Agrawal, W. N. Stiegelmeyer, and W. E. Berry, “Stress Corrosion Cracking Evaluation of ASTM A537 Steel in Simulated Radioactive Waste Solution at 180°C” From Batelle Columbus Laboratories to E. I. Dupont, January 19, 1983.
23. B. J. Wiersma and K. H. Subramanian, “Corrosion Control Measures for Liquid Radioactive Waste Storage Tanks at the Savannah River Site”, Journal of Nuclear Materials Management, July 2013.
24. J. A. Donovan and R. S. Ondrejcin to A. A. Kishbaugh, "Relative Resistance to Nitrate Cracking of A537 Class I and A516 Grade 70 Normalized Steels", March 23, 1977.
25. J. A. Donovan, "Resistance of Type A-537 Class I Steel to Nitrate Stress Corrosion Cracking", DPST-81-687.
26. K. H. Subramanian, “Vapor Corrosion Response of Low Carbon Steel Exposed to Simulate High Level Radioactive Waste”, WSRC-TR-2005-00508, Rev. 0, January 26, 2006.
27. K.H. Subramanian, “Review of Type I High Level Waste Tank Ultrasonic Inspection Data,” WSRC-TR-2003-00560,” December 2003.
28. K. H. Subramanian and P. E. Zapp, “Investigation of the Corrosivity of the Vapor Phase Over High Level Radioactive Waste”, CORROSION/2003, Paper No. 03676, NACE International, Houston, TX, 2003.
29. K. H. Subramanian and J. I. Mickalonis, “Anodic Polarization Behavior of Low Carbon Steel in Concentrated Sodium Hydroxide Solutions with Sodium Nitrate Additions, Electrochimica Acta, December, 2004.
30. K. H. Subramanian and B. J. Wiersma, “Vapor Space and Liquid/Air Interface Corrosion of Low Carbon Steel in Complex Radioactive High Level Waste”, CORROSION/2006, Paper No. 06637, NACE International, Houston, TX, 2006.
31. K. H. Subramanian and B. J. Wiersma, “High Level Waste Tank Farm Vapor Space Corrosion Program Zero-Step Implementation”, SRNL-MTS-2006-00078, Rev. 0, June 12, 2006.
32. R. S. Ondrejcin and E. J. Majzlik, "Galvanic and Crevice Corrosion of Pitted Waste Tanks: Review of A. D. Little Task 1 Interim Report Part 1", DPST-81-207, January 14, 1981.
33. R. S. Ondrejcin, "Pitting of New Nuclear Waste Tanks Galvanic Corrosion of Primary Liner", DPST-

81-410, May 6, 1981.
34. R. S. Ondrejcin and D. A. Mezzanotte, "Mechanism of Waste Tank Pitting", DPST-81-591, July 21, 1981.
35. R. L. Sindelar and B. J. Wiersma, “SRS High Level Waste Tank and Piping Systems – Structural Integrity Program and Topical Report”, WSRC-TR-95-0076, June 1995.
36. B. J. Wiersma, "Cooling Coil Failure Rates in Type I, II, and III Waste Tanks From 1970-92 (U)", SRT-MTS-92-3118, December 4, 1992.
37. R. S. Ondrejcin, "Investigation of Cooling Coil Corrosion in Radioactive-Waste Storage Tanks", DP-1425, January 1977.
38. S. P. Springer, "Tank 16 Cooling Coil Sections", 200-H Area Metallurgical Report, February 8, 1979.
39. B. J. Wiersma, "Measurement of the Ductile to Brittle Transition Temperature for Waste Tank Cooling Coils (U)", WSRC-TR-92-444, September 1992.
40. B. J. Wiersma, "Investigation of the Corrosion Behavior of Cooling Coil Material in a Simulated Concrete Environment",WSRC-TR-93-078, February 1, 1993.
41. B. J. Wiersma and M. S. Shurrab, "A Visual Assessment of the Concrete Vaults which Surround Underground Waste Storage Tanks (U)", WSRC-TR-93-761, December 1993.
42. R. S. Ondrejcin, "Inhibitors in Nuclear Waste Tank Cooling Coils (U)",WSRC-TR-91-37, January 18, 1991.
43. C. F. Jenkins, "Vapor Leak Repair, Tank 38H", 200-F&H Area Metallurgical Report, June 3, 1982.
44. C. F. Jenkins, "Defective Cooling Coil, Tank 43", 200-F&H Area Metallurgical Report, August 5, 1980.
45. C. F. Jenkins, "Defective Cooling Coil, Tank 44", 200-F&H Area Metallurgical Report, January 12, 1982.